ANALYSIS OF GPS DATA COLLECTED ON THE GREENLAND ICE SHEET[1]

Kristine M. Larson and John Plumb
Department of Aerospace Engineering Sciences, University of Colorado, Boulder, Colorado 80309

Jay Zwally
NASA Goddard Space Flight Center, Mailstop 971.0, Greenbelt, Maryland 20771

Waleed Abdalati
NASA National Headquarters, Washington, DC 20546-0001

Abstract: For several years, GPS observations have been made year round at the Swiss Camp, Greenland. The GPS data are recorded for 12 hours every 10–15 days; data are stored in memory and downloaded during the annual field season. Traditional GPS analysis techniques, where the receiver is assumed not to move within a 24-hour period, are not appropriate at the Swiss Camp, where horizontal velocities are on the order of 30 cm/day. Comparison of analysis strategies for these GPS data indicate that a parameterization can be chosen that minimizes noise due to satellite outages without corrupting the estimated ice positions. Low-elevation-angle observations should be included in the analysis in order to increase the number of satellites viewed at each data epoch. Carrier phase ambiguity resolution is important for improving the accuracy of receiver coordinates.

INTRODUCTION

GPS observations on the Greenland ice sheet are generally restricted to campaign-style measurements made during the summer field season. By comparison of measurements made in different years, the annual average velocity of locations on the ice sheet can be determined with a precision of better than 10 cm/yr (Thomas et al., 2000). In order to investigate the variability of ice flow velocities, continuous or quasi-continuous GPS measurements are required. While continuous GPS measure-

[1]We thank Koni Steffen for logistical support at the Swiss Camp. This research was supported by NASA grants to the University of Colorado and Goddard Space Flight Center. The University NAVStar Consortium (UNAVCO) provided technical assistance. We thank the Jet Propulsion Laboratory, the National Geodetic Survey, Kort & Matrikelstyrelsen (KMS), and Bundesamt für Kartographie und Geodäsie for supporting continuous GPS observations at Kulusuk (KULU), Thule (THU1), Kellyville (KELY), Scoresbysund (SCOB), and Reykjavik (REYK), respectively. Data for THU1, KELY, and REYK are freely available via anonymous ftp from the International GPS Service, or IGS (igscb.jpl.nasa.gov). Data from KULU and SCOB are available from UNAVCO (www.unavco.ucar.edu.) and KMS (forskning.kms.dk), respectively.

Polar Geography, 2001, **25**, No. 1, pp. 22-40.

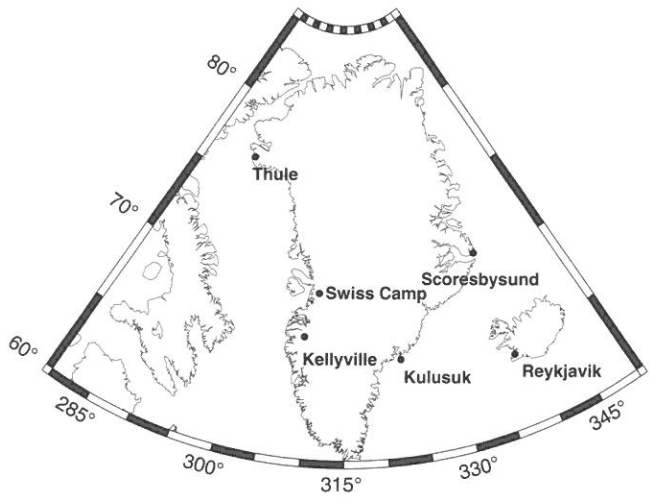

Fig. 1. Continuously operating GPS sites in Greenland and Iceland.

ments have been made in Greenland since 1995, the receivers generally have been on bedrock rather than the ice (Fig. 1). These sites were installed for investigations of solid Earth phenomena and/or support of GPS orbit determination. The horizontal motions of the bedrock sites are on the order of 1 cm/yr, which is consistent with the predictions of global plate motions for North America (Argus and Gordon, 1991). There is generally little significant nonlinear motion at permanent bedrock sites in Greenland (van Dam et al., 2000).

The speed of ice flow in Greenland is 3–4 orders of magnitude larger than tectonic motions observed on bedrock, depending on where observations are made (Thomas et al., 2000). Unlike tectonic motions, which are generally steady, it is not clear that surface velocities at different locations on the ice sheet are or should be constant. Observations of interannual variations in ice flow velocities would provide valuable insight about the flow characteristics that may be linked to seasonal parameters.

In 1996, an experiment was begun to measure variations in ice flow velocity near the Swiss Camp (Fig. 1). Established in 1990 at the nominal equilibrium line, the Swiss Camp has provided an extensive record of climatological variables and input for energy balance models (Steffen and Box, 2001). Because the equilibrium line is the boundary between areas of net mass gain (accumulation) and net mass loss (ablation), ice sheet behavior in this vicinity is of great interest. Morever, the existing infrastructure and extensive ancillary data make the site particularly well suited for a geodetic study of the ice sheet.

INSTALLATION AT SWISS CAMP

A dual-frequency GPS antenna was mounted on a 4 m long (0.09 m outer diameter) pole that was placed into a 2 m deep hole drilled into the ice. This left 2 m extending above the ice (Fig. 2) to ensure that the antenna would remain above any

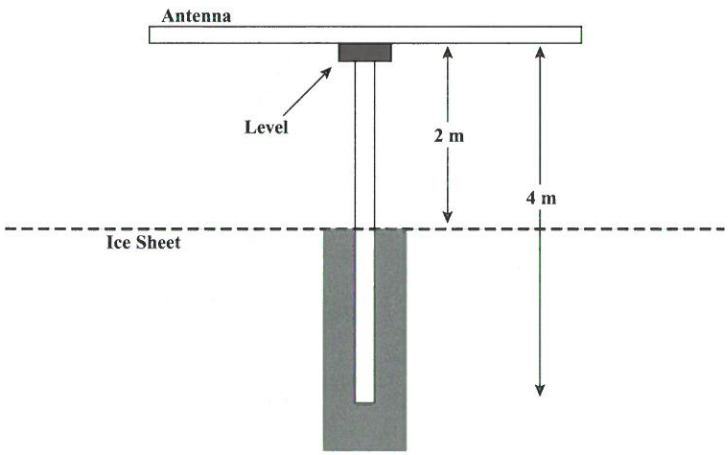

Fig. 2. The antenna installation at Swiss Camp.

snow accumulation that would occur during the measurement period. As measured over the previous five years, snow accumulation has been typically between 1 and 1.5 m at this site. The pole was aligned vertically using a level and then frozen into the ice for stability. Attached to the top of the pole is a specially designed leveling/mounting device that allows for easy leveling and orientation of the antenna; it is made very secure once the antenna is mounted. The receiver was placed inside an insulated protective box about 4 m from the antenna. The system was powered by four to six batteries and connected to two 18 W solar panels.

While satellite communication is possible at the Swiss Camp, power consumption for transmitting the GPS data would be much greater than capabilities that existed when this project began. Thus the GPS data were stored in the receiver's memory and were recovered during the annual field season in May–June. Likewise, while the GPS receiver used in this project is capable of continuous observations, there was not sufficient power and storage space available; instead quasi-continuous measurements were made, at intervals that will be discussed below. A Trimble 4000 SSi unit was purchased and upgraded from 5 to 40 Mbytes of internal memory so that an entire field season's results could be stored in it. Many geodetic GPS users cover antennas with a plastic dome to avoid build-up of snow (and dirt) on the antenna element. A protective dome was not installed at the Swiss Camp because wind is sufficient to remove snow from the antenna. The GPS receiver was programmed to make observations for 12 hours at regular intervals. The spacing and length of the surveys was limited by availability of sunlight to power the batteries as well as internal memory to store the measurements. Winter measurements were made at 15-day intervals, while measurements the rest of the year were made at 10-day intervals.

Although the average daily Swiss Camp velocity is much larger than most of the limiting error sources in GPS, the receiver was programmed in such a way to eliminate the effects of two particular error sources: constellation geometry and multipath. The GPS satellites have ground tracks that repeat with a sidereal period. In other words, an identical constellation is in view for 23 hours 56 minutes after the first

measurements. In practice, some satellites might not be available from day to day because that satellite might be turned off or maneuvered by the Department of Defense. Synchronizing the observations also helps to reduce the error resulting from multipath. While multipath errors are not eliminated by synchronizing measurements, their impact is reduced because the same multipath environment should be seen from day to day.

Which 12 hours of data should be collected during each 24-hour period? Generally a time period when the most satellites are visible should be used. Another concern is the geometric coverage of the satellite constellation. Satellites should be observed from all portions of the sky—i.e. north-south-east-west, and from low to high elevation angles. Even if the same number of satellites are being tracked by a receiver, the precision of the estimated receiver position can vary significantly depending on where the satellites are in the sky. For example, tracking eight satellites that are all at elevation angles between 15° and 25° will yield a less precise solution than tracking eight satellites distributed more evenly between elevation angles of 15° and 90°. Geodesists have developed a mathematical expression to predict the "goodness" of a particular satellite distribution. First, the variance-covariance matrix of the GPS position estimates are computed based on the partial derivative matrix used to derive the normal equations. Then the square root of the sum of the position variances is defined at each measurement epoch. This mathematical expression is called the position dilution of precision (PDOP):

$$PDOP = \sigma_x^2 + \sigma_y^2 + \sigma_x^2, \quad (1)$$

where σ_x^2, σ_y^2, and σ_x^2 are the unweighted Cartesian coordinate variances (Hoffmann-Wellenhof et al., 2001). PDOP gives the average position standard deviation. Figure 3 shows PDOP for the Swiss Camp in July 1998, with an annotation to denote the hours that were used for this study. Note that this window avoided several large PDOP spikes earlier in the 24-hour period. These large PDOP values are generally associated with times when the number of visible satellites was reduced.

GPS ANALYSIS

With the creation and expansion of the International GPS Service (IGS) (Beutler et al., 1994), and its associated analysis centers, it has become far easier for polar scientists to use GPS for precise applications such as the one described in this paper. The IGS uses a global tracking network to estimate very precise GPS orbits and Earth orientation parameters. This network is also used to determine precise coordinates that are used to define the International Terrestrial Reference Frame (ITRF97) (Boucher et al., 1999). Positions of the Swiss Camp were estimated with respect to ITRF97.

The GPS observations from Swiss Camp were analyzed using the GIPSY software developed at the Jet Propulsion Laboratory (JPL) (Lichten and Border, 1987). Both the pseudorange and carrier phase data are used in GIPSY solutions, although the precision of the coordinate estimates are controlled by the more precise carrier

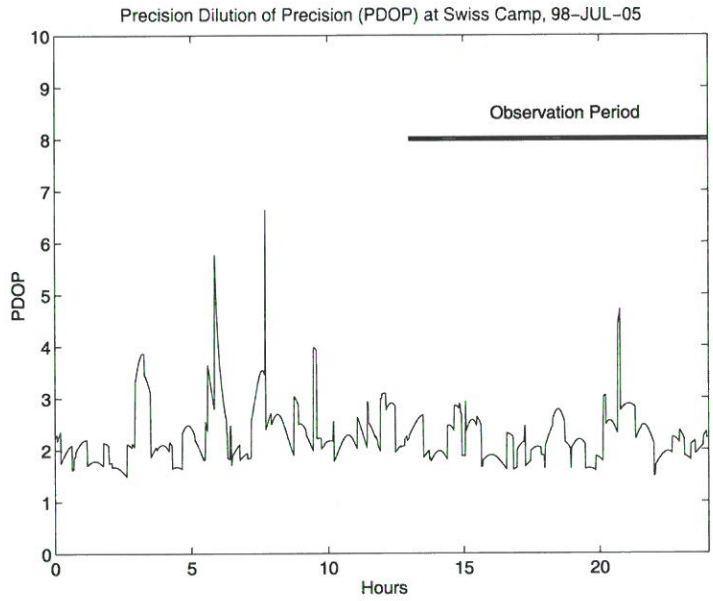

Fig. 3. Position Dilution of Precision (PDOP) for all satellites above an elevation-angle cut-off of 10° at the Swiss Camp, July 5, 1998.

phase observations. The carrier-phase and pseudorange observables, ϕ_r^s and P_r^s for a given satellite s and receiver r on a given frequency L_1 or L_2, can be written as:

$$\phi_{1r}^{s}\lambda_1 = \rho_g - c\delta^s + c\delta_r + \rho_{trop} - \rho_{1ion} + \rho_{mult}^{\phi 1} + N_{1r}^{s}\lambda_1 + \varepsilon_{\phi 1} \qquad (2)$$

$$\phi_{2r}^{s}\lambda_2 = \rho_g - c\delta^s + c\delta_r + \rho_{trop} - \rho_{2ion} + \rho_{mult}^{\phi 2} + N_{2r}^{s}\lambda_2 + \varepsilon_{\phi 2} \qquad (3)$$

and

$$P_{1r}^{s} = \rho_g - c\delta^s + c\delta_r + \rho_{trop} + \rho_{1ion} + \rho_{multi}^{P1} + \varepsilon_{p1} \qquad (4)$$

$$P_{2r}^{s} = \rho_g - c\delta^s + c\delta_r + \rho_{trop} + \rho_{2ion} + \rho_{mult}^{P2} + \varepsilon_{p2}, \qquad (5)$$

where λ_1 and λ_2 are the L_1 and L_2 carrier wavelengths; ρ^g is the geometric range, defined as $\left|\vec{X}^s - \vec{X}_r\right|$; $\vec{X}^s$ is the satellite position at the time of signal transmission;

$\vec{X}_r$ is the receiver position at reception time; δ_r and δ^s are the receiver and satellite clocks, respectively; and c is the speed of light. ρ_{trop} and ρ_{ion} are the propagation delays caused by the troposphere and ionosphere; ρ_{mult} describes multipath errors; and N^s_{1r} and N^s_{2r} are the carrier-phase ambiguities or biases. When the GPS receiver first "locks" onto the GPS signal, it can very precisely measure the fractional phase of the signal, but it does not know how many cycles it took to travel from the satellite to the receiver. This ambiguity must be estimated from the observations. ε_p and ε_ϕ are noise terms for the pseudorange and carrier phase observables, respectively. All terms of the observables equations, except clocks (seconds) and carrier phase biases, are defined in distance units.

Continuously operating GPS receivers generally report measurements at a higher rate than are later used to estimate positions. The Swiss Camp receiver produced observations at 15-second intervals, but the data were later decimated to 5-minute intervals when positions were estimated. This is done primarily to reduce the computational burden. This is appropriate when receiver motions (on the order of cm/hr) are small compared to the observation period (5 minutes). The higher-rate data are helpful for resolving cycle slips, which occur when a receiver loses track of the number of integer cycles that have passed since its last observation. For example, assume that a one wavelength cycle slip has occurred on L_2, ~24 cm. Algorithms that attempt to detect this cycle slip must ascertain whether the ionosphere could produce a change of 24 cm in the time between observations, or it is truly a cycle slip. It is much easier to bound the ionospheric variation over 15 seconds than over 5 minutes.

It is important to "fix" as many cycle slips as possible so that extra carrier phase biases do not have to be estimated. The great majority of cycle slips occur on L_2 because the Defense Department currently restricts access to the pseudorange data on this frequency. While current receiver technology has made great advances in reconstructing pseudorange measurements on the L_2 frequency, cycle slips still occur, particularly in regions where the ionosphere is most active—e.g., the equator and the higher latitudes.

The observable equations highlight that the ionospheric delay is frequency dependent. The magnitude of the effect is the same for pseudorange and carrier phase, but opposite in sign. To first order, $\rho_{ion} \sim TEC/f^2$, where TEC is the total electron content along the satellite-receiver path. The ionosphere free observables are formed in a way to remove this ionospheric dependence, and are often called the L_3 observables:

$$P^s_{3r} = \frac{f_1^2}{f_1^2 - f_2^2} P^s_{1r} - \frac{f_2^2}{f_1^2 - f_2^2} P^s_{2r} \tag{6}$$

and

$$\phi^s_{3r} = \frac{f_1^2}{f_1^2 - f_2^2} \phi^s_{1r} \lambda_1 - \frac{f_2^2}{f_1^2 - f_2^2} \phi^s_{2r} \lambda_2 . \tag{7}$$

TABLE 1

Summary of GPS Parameter Estimation Strategy

Model/parameter	Values/reference/estimation
Data interval	5 minutes
Elevation-angle cut-off	10°
Geopotential	JGM3 degree and order 12
Precession	IAU 1976 precession theory
Nutation	IAU 1980 nutation theory
Earth orientation	International Earth Rotation Service Bull. B
Yaw attitude	Bar-Sever (1996)
Ephemerides	IGS precise orbits, Beutler et al. (1994)
Reference clock	Thule
Pseudorange standard deviation	100 cm
Carrier-phase standard deviation	1 cm
Satellite clock	White noise, 1 sec.
Receiver position, Swiss Camp	Random walk
Receiver clock	White noise, 1 sec.
Phase ambiguity (real-valued)	Constant, 0.1 km
Zenith troposphere delay	Random walk, 1 cm/$\sqrt{\text{hour}}$

Along with the data from Swiss Camp, data from the other sites in Greenland (Fig. 1) were analyzed as well, although the positions of these sites were not allowed to vary within any 24-hour period.

The GPS parameter estimation strategy used is summarized in Table 1. The constraints used for the carrier phase ambiguities, clocks, and troposphere (N_r^s, δ_r, δ^s, and ρ_{trop}) are identical to those used for global plate motion (Larson et al., 1997) and time-transfer studies (Larson and Levine, 1999) except for the treatment of Swiss Camp's coordinates. The satellite orbits ($\vec{X}^s$) and Earth orientation parameters were fixed to values provided by the IGS and the International Earth Rotation Service, respectively.

We investigated the possibility of using JPL's precise point positioning technique (Zumberge et al., 1997). This analysis strategy has the advantage that only the data from Swiss Camp need to be analyzed. A major disadvantage is that the resulting solution does not allow for ambiguity resolution (Blewitt, 1989), which requires data from two or more GPS receivers. In a later paper, we will demonstrate the importance of ambiguity resolution in estimating time-varying station coordinates.

RECEIVER COORDINATES

In many geophysical applications it can be assumed that GPS receivers do not move during the 24-hour observing period. The GPS analysis software then estimates a single position for the observing period. This assumption is clearly not valid in the

cases of active volcanoes (Owen et al., 2000) and ice sheets. Another simple model that could be used is allowing the receiver coordinates to vary linearly in time. Doing so makes a very rigid assumption about the processes that move the Earth's surface, but it might be valid for certain applications. A more sophisticated model allows the receiver coordinates to change with time, using statistical constraints to impose, for example, smoothness in the receiver coordinates over time. This latter approach has been adopted in this paper to minimize the assumptions made about the processes that move the ice sheets. By allowing the receiver coordinates to vary in time with statistical constraints, it is also possible to assess the impact of satellite outages on the position estimates.

In principle it is simple to vary receiver coordinates in GIPSY, which allows time-varying processes to be modeled as a "white noise" process, with no temporal correlation, a random walk process with infinite correlation, or with more general Gauss-Markov processes with intermediate correlation lengths. Results were compared using different correlation lengths; they were found to be no more precise or accurate than a random walk model, so the focus of this paper is the random walk model. For comparison, white noise coordinate estimates were also estimated.

For a random walk, the position of the GPS receiver, **x**, is defined as:

$$\mathbf{w_{k+1}} = \mathbf{x_k} + \mathbf{w_k}, \tag{8}$$

where $\mathbf{w_k}$ is a vector of normally distributed zero-mean random perturbations and the indices k+1 and k refer to increments in time. The variance of the i-th component of the process noise **w** is:

$$\langle w_i\,(t)^2\rangle = q\Delta t = \sigma^2_{rw}\,\Delta t; \tag{9}$$

q then is the variance per unit time and generates the random walk (Technical Staff, 1974). In the GIPSY software, $\sqrt{q}$ is an input; the units of this parameter are km/$\sqrt{\text{sec}}$. Following the GIPSY notation, $\sqrt{q}$ will be referred to as σ_{rw}; the units will always be defined as above.

A value of σ_{rw} needs to be chosen that is appropriate for the time scales found in the data. One must first assess how much the positions vary in time. For many geophysical applications, temporal variability is small—e.g., positions move 0.1 to 10 cm/hr. A σ_{rw} value for these time scales should be chosen in such a way as to minimize noise in the estimates. If σ_{rw} is too small, the position estimates will be biased toward no motion. In any case, a σ_{rw} chosen for slow-moving geophysical applications would not be appropriate for other GPS filtering applications, such as for data collected on a moving aircraft. In the latter case, white noise estimation would be appropriate.

ANALYSIS AND DISCUSSION OF SCORESBYSUND DATA

The selection of the optimal σ_{rw} value for Swiss Camp is complicated by the fact that while the ice is moving, we do not know its velocity exactly and we cannot be sure that the velocity in summer, for example, is the same as the velocity in winter. Ideally we would like to test our filtering strategy on a data set collected with the

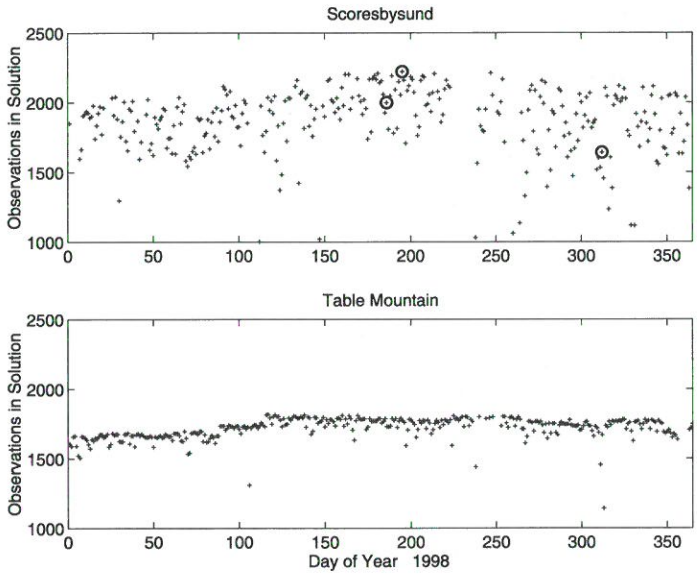

Fig. 4. Number of observations used in a 24-hour GIPSY solution for Scoresbysund and Table Mountain. Scoresbysund is located at a latitude of 70.48° N; Table Mountain is located at a latitude of 40.13° N. Three days are circled and are discussed in the text.

same satellite geometry as Swiss Camp but with exact knowledge of how rapidly the receiver (or ice) moved. Scoresbysund (Fig. 1) is ideally located for testing Swiss Camp filtering strategies, as its latitude (70.48° N) is similar to that of Swiss Camp (69.57° N). Unlike Swiss Camp, it is continuously operating and can be used to assess the impact of "data quality" on position estimates over an entire year.

Figure 4 is indicative of data quality problems associated with high-latitude sites. The number of observations collected for a year are plotted for two sites: Scoresbysund and Table Mountain, Colorado (40.13° N). While the mean number of observations used in the Scoresbysund solution is significantly higher than at Table Mountain, this simply reflects the fact that a 12-channel receiver has been installed at Scoresbysund, and the Table Mountain receiver is an older model, 8-channel receiver. The number of channels relates to the number of satellites that can be tracked at any given time. The Table Mountain receiver tracks fewer satellites, but it does so much more consistently. The slight change in observations around day 120 is the result of adding a new GPS satellite (PRN08) to the solution. Although this satellite was launched in late 1997, several months must pass before a new satellite is declared operational and used in IGS orbit solutions.

The GPS antenna at Scoresbysund has been installed on bedrock and should move less than 0.1 mm in a 24-hour period. While we could investigate the ability to measure null velocities at Scoresbysund, the filtering strategy could be inadvertently biased—i.e., a small σ_{rw} could produce a velocity of 0 cm/hr, but not a larger velocity like 1 cm/hr. Elosegui et al. (1996) built an apparatus that moved a GPS antenna at a predefined velocity, 1 mm/hr, and then varied their filtering strategy to see which best recovered the given antenna velocity. Alternatively, estimation strategies can be

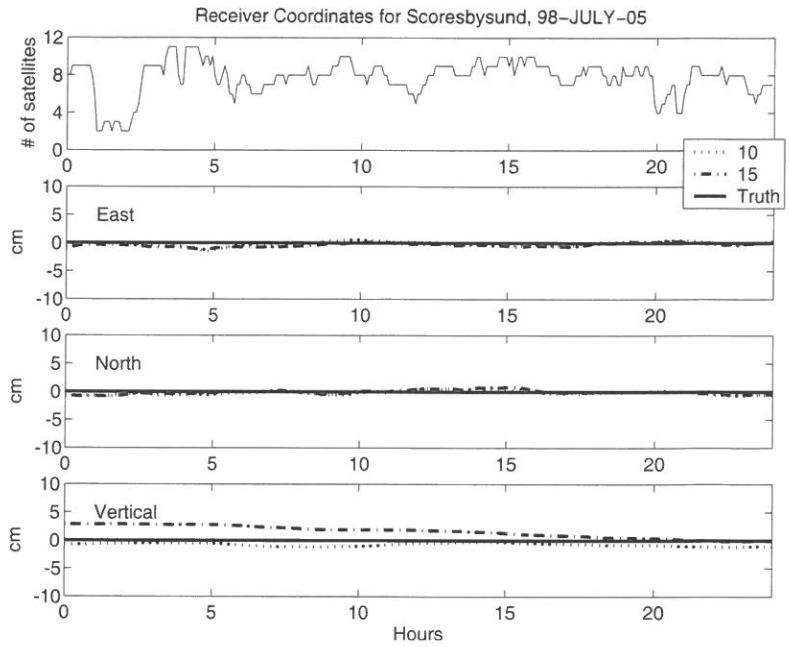

Fig. 5. Residual receiver coordinates for Scoresbysund, July 5, 1998. The *a priori* velocity has been removed, so that perfect agreement is shown at zero. Scoresbysund solutions are shown for elevation-angle cut-offs of 10° and 15°.

tested using observations from Scoresbysund with a simulated *a priori* velocity. In each case tested here, the *a priori* receiver position is defined to move horizontally by 30 cm/day. When the receiver position is subsequently estimated, it should move at a velocity that is the negative of the input velocity, since the Scoresbysund receiver did not actually move.

Several Scoresbysund solutions have been highlighted in Figure 4. These will be used to illustrate some of the features in the data, particularly as they relate to data quality and varying filtering strategies. In each case the number of visible satellites above a 10° elevation cutoff is shown. An *a priori* velocity of 30 cm/day was input into the horizontal receiver coordinates, and subsequently that same signal was removed so that the residual position estimates could be inspected (Fig. 5). In this case σ_{rw} was defined as 10^{-7} km/$\sqrt{\text{sec}}$. The two numerical solutions shown used different elevation-angle cutoffs. For many years a 15° elevation-angle cutoff was used in many geodetic analyses (Lichten and Border, 1987; Blewitt, 1989), although others used even higher cutoffs, e.g. 20°. Most cycle slips occur at lower elevation angles, and the data are, in general, noisier because of multipath. It is also more difficult to accurately correct the tropospheric delay at the lower elevation angles. For all these reasons, lower-elevation data are frequently discarded. Subsequent work has shown that a more reliable vertical estimate can be determined by using lower elevation-angle data (Bar-Sever et al., 1998). This was also the case for the kinematic simulation for Scoresbysund. Inclusion of the lower elevation-angle data has little influence on the horizontal velocities but has a pronounced impact on the vertical velocity. The

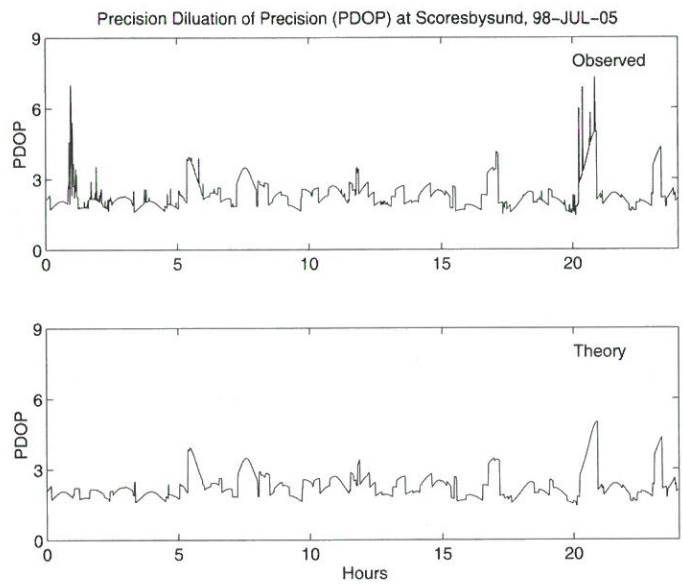

Fig. 6. Position Dilution of Precision (PDOP) at Scoresbysund, July 5, 1998.

slope of the vertical displacement (bottom panel of Fig. 5) is reduced from -3.4 cm/day to -0.2 cm/day by using an elevation-angle cutoff of 10°, which significantly improves the agreement with the *a priori* velocity of 0 cm/day.

The top panel of Figure 5 shows a significant data outage in the first three hours of data. This could be a real satellite outage or could be related to the quality of receiver tracking on July 5, 1998. PDOP is calculated in Figure 6 for both the actual number of satellites that were broadcasting on that day and the satellites actually observed by Scoresbysund. It is apparent that the receiver had great difficulty tracking at approximately 01:00 UTC. This will, in general, result in poorer ability to resolve position and velocity.

Figure 7 shows Scoresbysund solution results for November 8, 1998. On this particular day there were approximately 20% fewer observations than on July 5, 1998, with most of the data outage concentrated in the first six hours of the data file. Again, the north component gives a fairly robust estimate of velocity, but there is a significant transient observed in the east component, which is directly related to the satellite outages in the early part of the day. For most locations on the Earth, the GPS satellites track preferentially north-south, which leads to weaker estimates of the east component, particularly when fewer satellites are in view.

Assuming that a sufficient number of satellites are available, we still have not resolved the issue of choosing an optimal value of σ_{rw}. The impact of varying σ_{rw} in the time domain is shown in Figure 8. For the white noise case, equivalent to a large σ_{rw} value, one can see that satellite outages have an enormous impact. As σ_{rw} is decreased, the noise features also become smaller. The tighter random walk constraints also produce more reasonable solutions during satellite outages. If the σ_{rw} constraint is tightened too much, the estimated velocity can significantly deviate from the

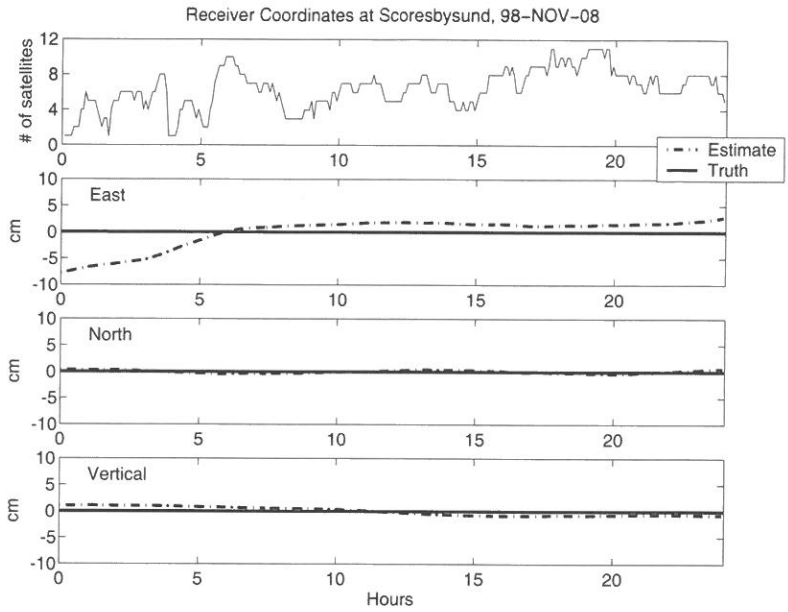

Fig. 7. Residual receiver coordinates for Scoresbysund, November 8, 1998. The *a priori* velocity has been removed, so that perfect agreement is shown at zero.

input velocity. The Scoresbysund filter test cases are summarized in Figure 9. In each case, solutions were computed for σ_{rw} values that vary by nearly three orders of magnitude. The solutions for very small σ_{rw}, e.g. 10^{-9}, incorrectly estimate a velocity of 0 cm/day. An accurate solution, 30 cm/day, is recovered at values of $7 \cdot 10^{-8}$ and above.

Each of the cases discussed above used 24 hours to resolve velocity. Because of memory and power limitations, only 12 hours of GPS data will be available at the Swiss Camp. It would be useful to determine how much data would be required to estimate an accurate velocity. In Figure 10 solutions are computed for three values of σ_{rw}—$7 \cdot 10^{-8}$, $1 \cdot 10^{-7}$, and $3 \cdot 10^{-7}$. The solutions are also computed using different lengths of time, ranging from 3 to 24 hours. Again, the north component needs fewer observations to correctly estimate the input velocity of 30 cm/day; the east component results suggest our observing period should have been a little longer than 12 hours, with converged solutions at 15 hours. We can use the misfit so as to properly estimate the velocity uncertainties computed for Swiss Camp.

In each of the cases shown above, carrier phase ambiguities were resolved. In GIPSY data processing, carrier phase ambiguities are first estimated as real-valued numbers. Since it is known theoretically that these ambiguities should be integers, if the values of those integers can be determined and "fixed," the parameters are essentially removed from the least squares estimation process. This reduces the number of unknowns to be estimated from the observations, and strengthens the solution of the remaining estimated parameters. The value of ambiguity resolution for static GPS applications has been long established (Blewitt, 1989; Dong and Bock, 1989) and it would be unexpected if ambiguity resolution did not improve the position estimates at Scoresbysund and Swiss Camp. For the sake of completeness, GPS position estimates

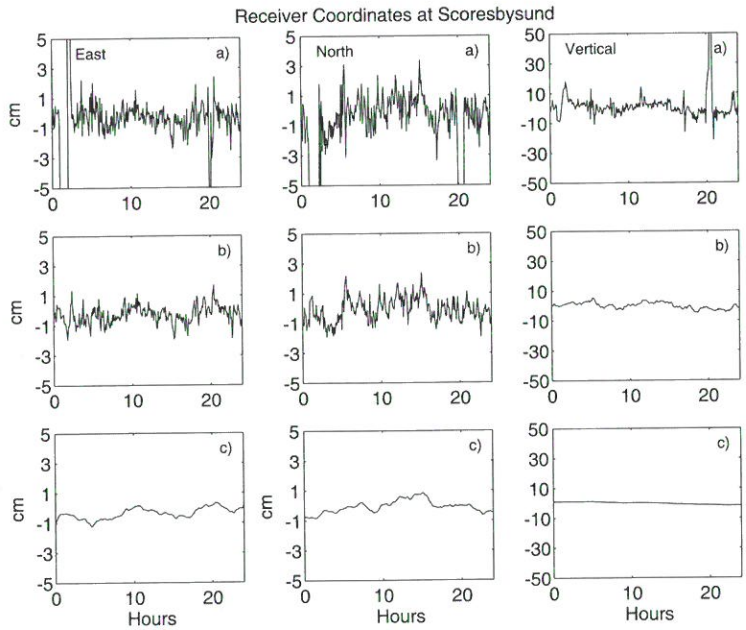

Fig. 8. A comparison of filter strategies for Scoresbysund, July 5, 1998, using white noise (A), random walk σ_{rw} of 10^{-6} (B), and 10^{-7} (C) km/$\sqrt{\text{sec}}$. Note change in scale for the vertical component. In each case the true velocity is 0 cm/hr.

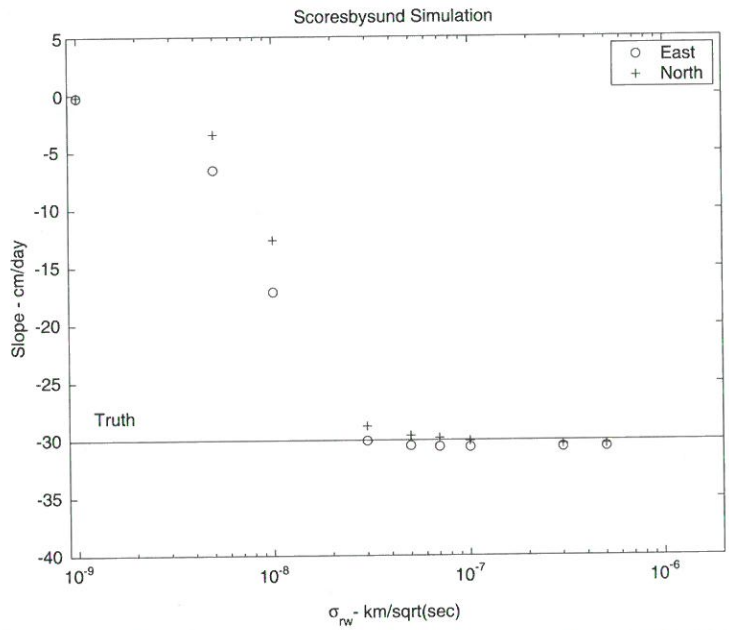

Fig. 9. Comparison of solution velocities for various σ_{rw} for Scoresbysund, July 14, 1998.

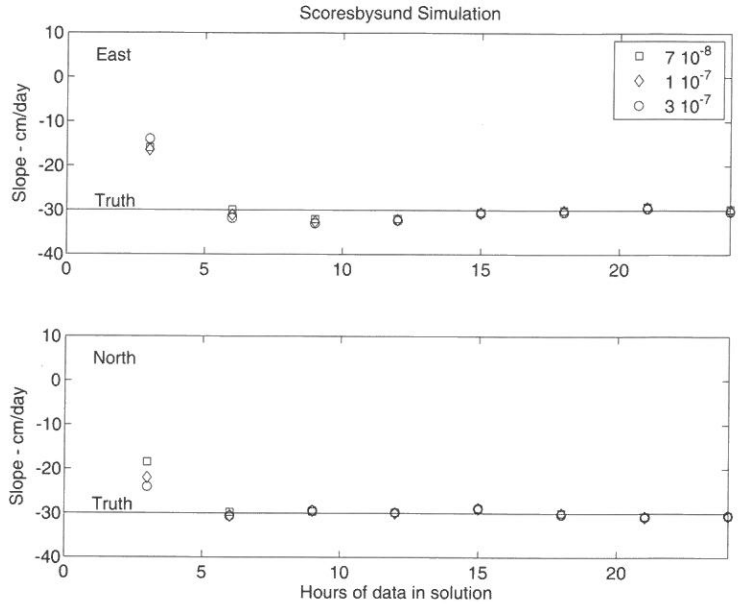

Fig. 10. Comparison of solution velocities as a function of hours of data used in the solution, Scoresbysund, July 14, 1998.

at Scoresbysund are shown in Figure 11, with and without ambiguity resolution. Clearly the position estimates for the east and vertical bias-free solutions disagree markedly with the *a priori* input, with little effect on the north component.

ANALYSIS AND DISCUSSION OF SWISS CAMP DATA

As noted previously, the Swiss Camp receiver was programmed to operate at regular intervals throughout the year, with more frequent operation in the spring-summer-fall. The number of usable observations is shown in Figure 12, for both 10 and 15° elevation-angle cutoffs. Data retrieval was fairly good, with only one day of observations lost due to complete receiver failure. On two days the receiver stopped tracking after 3–4 hours; no results are reported for these days. On three days it appears that no data below 15° were tracked by the receiver. After searching the database, it was discovered that on those three days the field crew inadvertently programmed the receiver to *not* track below 15°.

As at Scoresbysund, occasional data outages were observed in data collected at the Swiss Camp. The Swiss Camp solutions for August 4, 1998 are shown in Figure 13. By comparing these estimates with data collected only two weeks earlier, the satellite outages on August 4 can be clearly discerned. The impact of the satellite outages on August 4 can be observed in the white noise position estimates. Even with these data outages, a proper random walk estimation strategy (also shown in Figure 13) yields significantly smoother estimates, which agree well with estimates earlier in the day when a full constellation was tracked. The data outages on this day

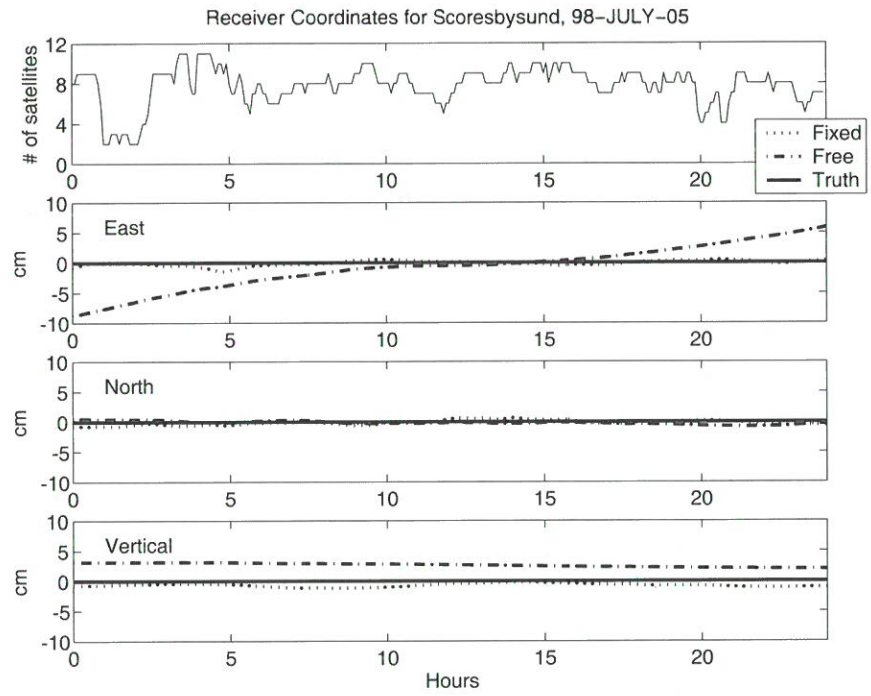

Fig. 11. Comparison of bias-fixed and bias-free solutions.

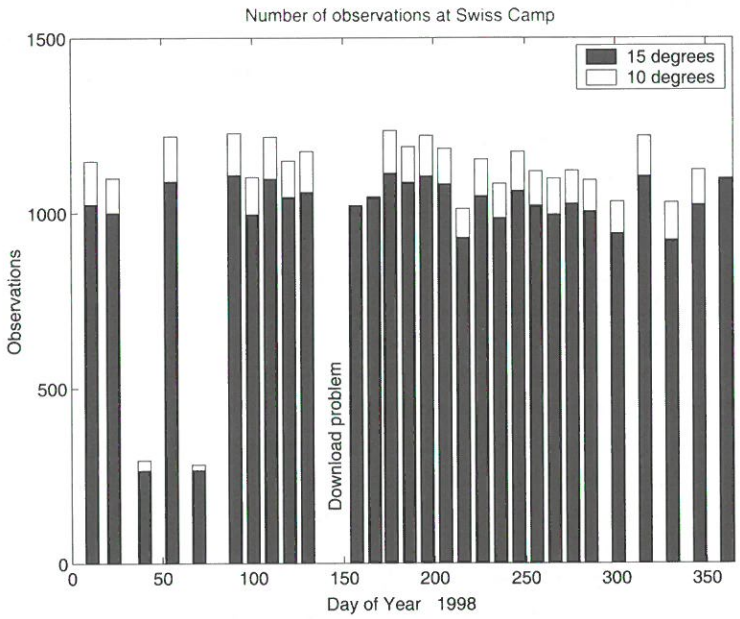

Fig. 12. Number of observations above 10° and 15° at Swiss Camp for 1998. Partially corrupted data files are seen for days 40 and 70; no data could be retrieved for day 146.

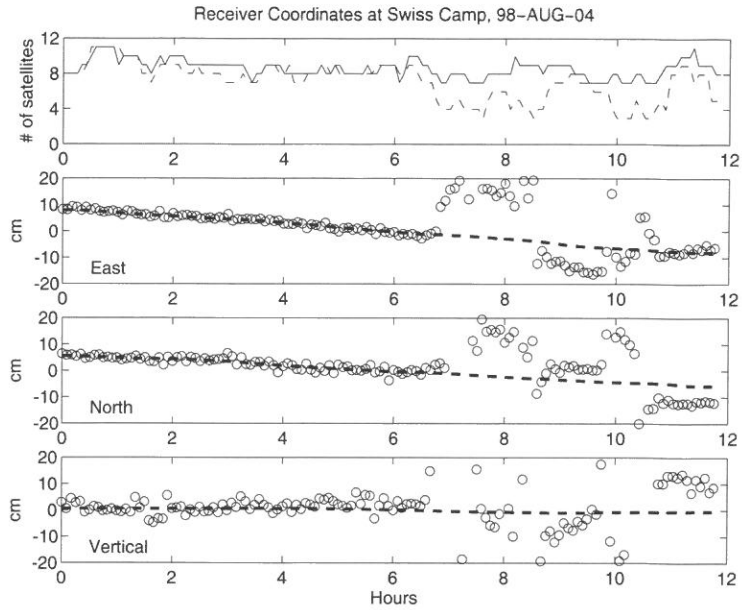

Fig. 13. Comparison of Swiss Camp positions for August 4, 1998. Two filter solutions are shown, a random walk estimation (dashed line) with σ_{rw} of 10^{-7} and an unconstrained white noise (open circles) solution. Note how the outliers in the white noise solution correlate with a low number of GPS satellites on August 4. For comparison, the number of satellites visible on July 15 (dashed line) are also shown in the first panel. An elevation cut-off of 10° was used and ambiguities were resolved in each case.

at Swiss Camp correspond to frequent loss of lock on the L_2 frequency. There was no corresponding difficulty in tracking L_2 on the other sites in Greenland on this day.

The coordinate results for one year of GPS data from the Swiss Camp are shown in east, north, and vertical coordinates in Figure 14. The direction of local ice flow motion can be determined by estimating the long-term trend in the east and north directions, with an average velocity of 31.8 ± 0.1 cm/day. The Swiss Camp is also dropping vertically at a rate of 0.6 ± 0.1 cm/day. After removing the linear trend from the position estimates, we can see the residual variation of Swiss Camp coordinates (Fig. 15). These position residuals show that there are significant variations in ice velocity that correlate with the seasons. Specifically, the maximum southwestward residual of more than 2 meters (relative to the position assuming constant horizontal velocity) indicates that the ice velocity accelerated up to 25% above the yearly average during the summer of this year. A discussion of this temporal variability in ice flow and the scientific implications is beyond the scope of this paper, but is given in Zwally et al. (in prep.).

CONCLUSIONS

It has been demonstrated that autonomous GPS systems can be successfully deployed on the Greenland ice sheet. In this experiment, solar cells and battery power

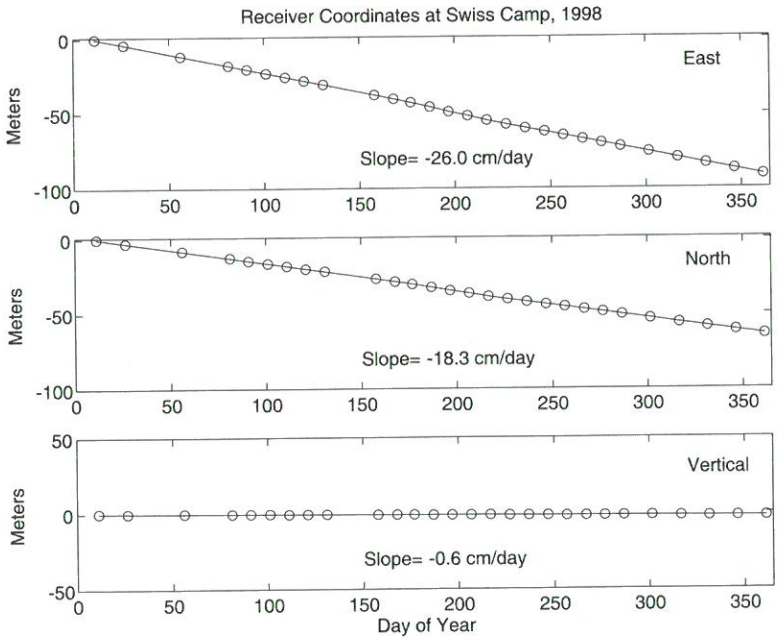

Fig. 14. Estimates of the Swiss Camp position, rotated into local east, north, and vertical directions. A best-fit straight line is also shown.

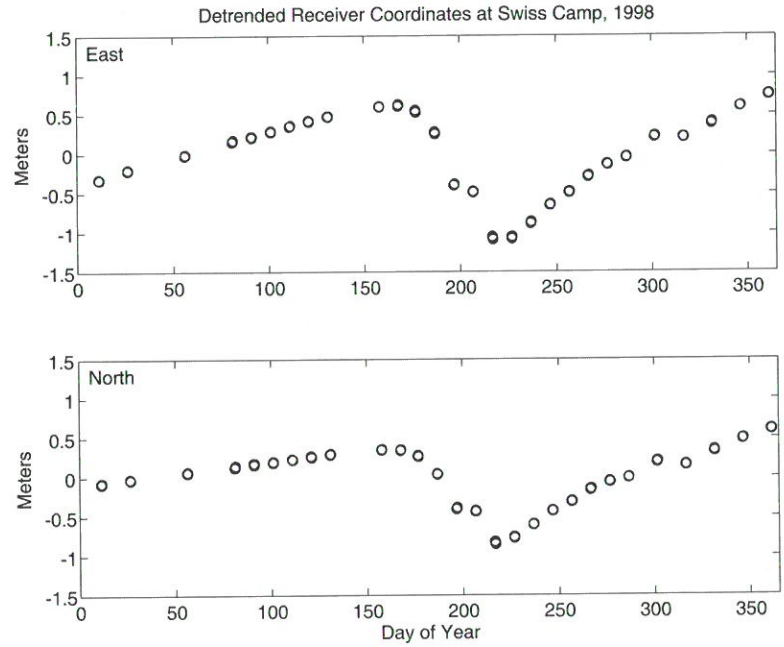

Fig. 15. Detrended estimates of the Swiss Camp position, rotated into local east and north directions.

were used to operate the equipment. Other investigators have tried to use wind power (in Antarctica), with much less success. The receiver used in this study appears to have operated with little difficulty in the extreme temperature environment.

Solutions computed at Scoresbysund demonstrate the value of tracking satellites at lower elevation angles. This suggests that older-model receivers (8 channels) should not be used; newer models that can track up to 12 satellites will result in more robust solutions.

LITERATURE

Argus, D. and R. Gordon. "No-net rotation model of current plate velocities incorporating plate motion model NUVEL-1," *Geophysical Research Letters*, Vol. 18, 1991, pp. 2039-2042.

Bar-Sever, Y. E. "A new model for GPS yaw attitude," in G. Gendt and G. Dick, eds., *Proceedings IGS Workshop: Special Topics and New Directions*. Potsdam, Germany, GeoForschungsZentrum, 1996, pp. 128-140.

Bar-Sever, Y., P. Kroger, and J. Borjesson. "Estimating horizontal gradients of tropospheric path delay with a single GPS receiver," *Journal of Geophysical Research*, Vol. 103, 1998, pp. 5019-5035.

Beutler, G., I. I. Mueller, and R. E. Neilan. "The International GPS Service for Geodynamics (IGS): Development and start of official service on January 1, 1994," *Bulletin Geodesique*, Vol. 68, 1994, pp. 39-70.

Blewitt, G. "Carrier phase ambiguity resolution for the Global Positioning System applied to geodetic baselines up to 2000 km," *Journal of Geophysical Research*, Vol. 94, 1989, pp. 10,187-10,203.

Boucher, C., Z. Altamimi, and P. Sillard. "The 1997 International Terrestrial Reference Frame (ITRF97)," *IERS Technical Note 27*. Paris, France: International Earth Rotation Service, 1999.

Dong, D. and Y. Bock. "Global Positioning System network analysis with phase ambiguity resolution applied to crustal deformation studies in California," *Journal of Geophysical Research*, Vol. 94, 1989, pp. 3949-3966.

Elosegui, P., J. Davis, J. Johansson, and I. Shapiro. "Detection of transient motions with the Global Positioning System," *Journal of Geophysical Research*, Vol. 101, 1996, pp. 11,249-11,261.

Hoffman-Wellenhof, B. *GPS: Theory and Practice*, fifth ed. New York, NY: Springer-Verlag, 2001.

Larson, K. M., J. Freymueller, and S. Philipsen. "Global plate velocities from the Global Positioning System," *Journal of Geophysical Research*, Vol. 102, 1997, pp. 9961-9982.

Larson, K. M., and J. Levine. "Carrier phase time transfer," *IEEE Transactions on Ultrasonics, Ferroelectronics, and Frequency Control*, Vol. 46, 1999, pp. 1001-1012.

Lichten, S. and J. Border. "Strategies for high precision GPS orbit determination," *Journal of Geophysical Research*, Vol. 92, 1987, pp. 12,751-12,762.

Owen, S., P. Segall, M. Lisowski, M. Murray, M. Bevis, and J. Foster. "The January 30, 1997 eruptive event on Kilauea Volcano, Hawaii, as monitored by continuous GPS," *Geophysical Research Letters*, Vol. 27, 2000, pp. 2757-2560.

Steffen, K., and J. Box. "Surface climatology of the Greenland ice sheet: Greenland climate network 1995–1999," *Journal of Geophysical Research*, Vol. 106, No. D24, 2001, pp. 33,951-33,964.

Technical Staff, The Analytic Sciences Corporation. *Applied Optimal Estimation* (Arthur Gelb, ed.). Cambridge, MA: The MIT Press, 1974.

Thomas, R., T. Akins, B. Csatho, M. Fahnestock, P. Gogineni, C. Kim, and J. Sonntag. "Mass balance of the Greenland ice sheet at high elevations," *Science*, Vol. 289(5478), 2000, pp. 426-428.

van Dam, T., J. Wahr, K. Larson, O. Francis, and S. Gross. "Using geodesy to observe ice mass changes," *EOS (Transactions of the American Geophysical Union)*, Vol. 81, No. 37, 2000, pp. 421-427.

Zumberge, J. F., M. B. Heflin, D. C. Jefferson, M. M. Watkins, and F. H. Webb. "Precise point positioning for the efficient and robust analysis of GPS data from large networks," *Journal of Geophysical Research*, Vol. 102, 1997, pp. 5005-5017.

Zwally, H. J., W. Abdalati, K. Larson, and K. Steffen. "Melt-induced acceleration of Greenland Ice Sheet flow," manuscript in preparation.